3D Orthogonal Woven Triboelectric Nanogenerator for Effective Biomechanical Energy Harvesting and as Self-Powered Active Motion Sensors

*Kai Dong, Jianan Deng, Yunlong Zi, Yi-Cheng Wang, Cheng Xu, Haiyang Zou, Wenbo Ding, Yejing Dai, Bohong Gu, Baozhong Sun, and Zhong Lin Wang**

The development of wearable and large-area energy-harvesting textiles has received intensive attention due to their promising applications in next-generation wearable functional electronics. However, the limited power outputs of conventional textiles have largely hindered their development. Here, in combination with the stainless steel/polyester fiber blended yarn, the polydimethylsiloxane-coated energy-harvesting yarn, and nonconductive binding yarn, a high-power-output textile triboelectric nanogenerator (TENG) with 3D orthogonal woven structure is developed for effective biomechanical energy harvesting and active motion signal tracking. Based on the advanced 3D structural design, the maximum peak power density of 3D textile can reach 263.36 mW m^{-2} under the tapping frequency of 3 Hz, which is several times more than that of conventional 2D textile TENGs. Besides, its collected power is capable of lighting up a warning indicator, sustainably charging a commercial capacitor, and powering a smart watch. The 3D textile TENG can also be used as a self-powered active motion sensor to constantly monitor the movement signals of human body. Furthermore, a smart dancing blanket is designed to simultaneously convert biomechanical energy and perceive body movement. This work provides a new direction for multifunctional self-powered textiles with potential applications in wearable electronics, home security, and personalized healthcare.

Smart textiles (electrical textiles)[1–4] have been considered as the next-generation wearable electronics due to their promising applications in vast fields ranging from self-powered devices,[5–7] physiological/wellness monitors,[8–10] wearable human-interactive interfaces,[11] to shape-adaptive military/consumer electronics.[12–14] As a result, various fiber-like or fabric-shaped components of miniature electronic devices have been demonstrated in smart garments or fabrics, such as organic light-emitting diodes (LEDs),[15] field-effect transistors,[16] artificial skin sensors,[17] and medical diagnosis.[18] As usual, the operations of these wearable electronics require an extra power source. Owing to the conventional bulky batteries lacking of the required flexibility, comfort and lightweight for textile, various kinds of fiber-based or fabric-based energy storage devices (lithium-ion batteries[19,20] and electrochemical supercapacitors[21,22]) have been integrated into textiles. However, these flexible energy-storing devices require frequent and inconvenient charging, which largely hinders the practical, sustainable, and broad-range applications of the wearable electronics.

As a continuous, self-sufficient and sustained power-supplying source, triboelectric nanogenerator (TENG) is a newly developed energy-harvesting technology that can convert ubiquitous mechanical energies into electric power with a coupled effect of contact-electrification and electrostatic induction.[23,24] Considering its low cost, high efficiency, environmental friendliness, and universal availability, it has promising applications in both small mechanical energy scavenging and large-scale energy generation. Especially, it shows obvious advantages in collecting low-frequency and irregular mechanical energies such as human motions,[25] wind,[26] water waves,[27] and vibration.[28] Due to the universal existence of triboelectricity, the materials' choice for the TENG is enormous,[23,24] which makes it feasible in designing a versatile deformable and wearable TENG for harvesting energy from human body and as self-powered active motion sensors.

The combination of emerging TENG technology and traditional textile technology brings more possibilities for self-powered textiles. However, the further advancement of self-powered textiles still faces several critical challenges. First and foremost, the power harvesting from conventional 2D woven (i.e., plain,

K. Dong, J. Deng, Dr. Y. Zi, Dr. Y.-C. Wang, Dr. C. Xu, H. Zou, Dr. W. Ding, Dr. Y. Dai, Prof. Z. L. Wang
School of Material Science and Engineering
Georgia Institute of Technology
Atlanta, GA 30332-0245, USA
E-mail: zhong.wang@mse.gatech.edu
K. Dong, Prof. B. Gu, Prof. B. Sun
College of Textiles
Key Laboratory of High Performance Fibers and Products
Ministry of Education
Donghua University
Shanghai 201020, P. R. China
Prof. Z. L. Wang
Beijing Institute of Nanoenergy and Nanosystems
Chinese Academy of Sciences
National Center for Nanoscience and Technology (NCNST)
Beijing 100083, P. R. China

DOI: 10.1002/adma.201702648

twill, and stain) TENGs[29–31] was not enough to actuate most of wearable electronics. The demand of self-powered textiles with high-power-output performances is extremely urgent. Second, a majority of fiber-like or fabric-shaped electrodes, such as metal,[19,29] grapheme,[32,33] carbon nanotubes,[34,35] and carbon nanofiber,[36] were obtained from complicated and time-consuming chemical treatment procedures (e.g., electroless deposition and electroplating), which were neither cost effective nor environmentally friendly. Besides, these procedures make the electronic textiles not washable due to loss of surface conductive materials. Third, most of textile TENGs rely on external substrates or surfaces to acquire sliding or contact-separating triboelectricity,[31,37,38] which limited the application field and scope of self-powered textile TENGs.

In this paper, a high-power-output 3D orthogonal woven TENG (3DOW-TENG) was designed by comparing the energy acquisition capacities of different textile structures as well as their corresponding circuit connection modes. The fabricated 3DOW textiles were machine washable, tailorable, breathable, aiming at harvesting the biomechanical energy and capturing the motion signals. The novel 3DOW textiles were fabricated from three types of yarns: 3-ply-twisted stainless steel/polyester fiber blended yarn (warp yarn), polydimethylsiloxane (PDMS)-coated energy-harvesting yarn (weft yarn), and binding yarns in thickness direction (*Z*-yarn). Under the tapping frequency of 3 Hz, the peak power density of our 3DOW-TENG could reach 263.36 mW m^{-2} with an external load resistance of 132 MΩ, which was several times more than that of conventional 2D textile TENGs.[6,29,30] Furthermore, a large-area 3DOW-TENG was fabricated to sustainably charge commercial capacitors and drive a digital watch. Our 3DOW textiles could also actively and sensitively monitor the movement signals of human body, which has a promising application in self-powered active motion sensors. Finally, with the high-power-output and active motion sensing performances of 3DOW-TENG, a self-powered dancing blanket was designed, which would have potential applications in future intelligence unlocking and home security protection. This work pushes the progress of high-power-output wearable textile TENGs for application in energy harvester and active motion sensor, which will shed light on the future developing direction of self-powered wearable textiles.

As we know, the triboelectric effect is a contact-induced electrification in which a material becomes electrically charged after it is contacted with a different material, and the sign of the charges to be carried by a material depends on its relative polarity in comparison to its counterpart.[23,24,39] Therefore, reasonable selection of the conductive and dielectric materials is crucial to achieve a high-power-output energy-harvesting textile. In this work, 3-ply-twisted stainless steel/polyester fiber blended yarn (surface resistance < 10^4 Ω, **Figure 1**a) was selected as the conductive electrode. This conductive yarn not only qualifies good electrical conductivity, but also keeps the comfortable ability of textile for wearable application, which was also discussed in detail (Note S1, Supporting Information). Considering that the good biocompatiblity, water-proof, and temperature insensitivity were desired for textiles, flexible yet tough PDMS was chosen as dielectric material. The energy-harvesting yarn was fabricated by coating PDMS on the 3-ply-twisted blended yarn. A specific device (Figure S1, Supporting Information) was designed to form the PDMS on the yarn and keep the thickness of PDMS uniformly. The detailed fabrication methods were discussed in the "Experimental Section" (Note S2, Supporting Information). With the help of this device, the blended yarns were almost warped in the center zone of the outer PDMS, as shown in Figure 1b. It is necessary to point out that the coating amount of PDMS on the conductive yarn (i.e., the diameter of the energy-harvesting yarn) has a significant influence on its power output. Therefore, different diameters

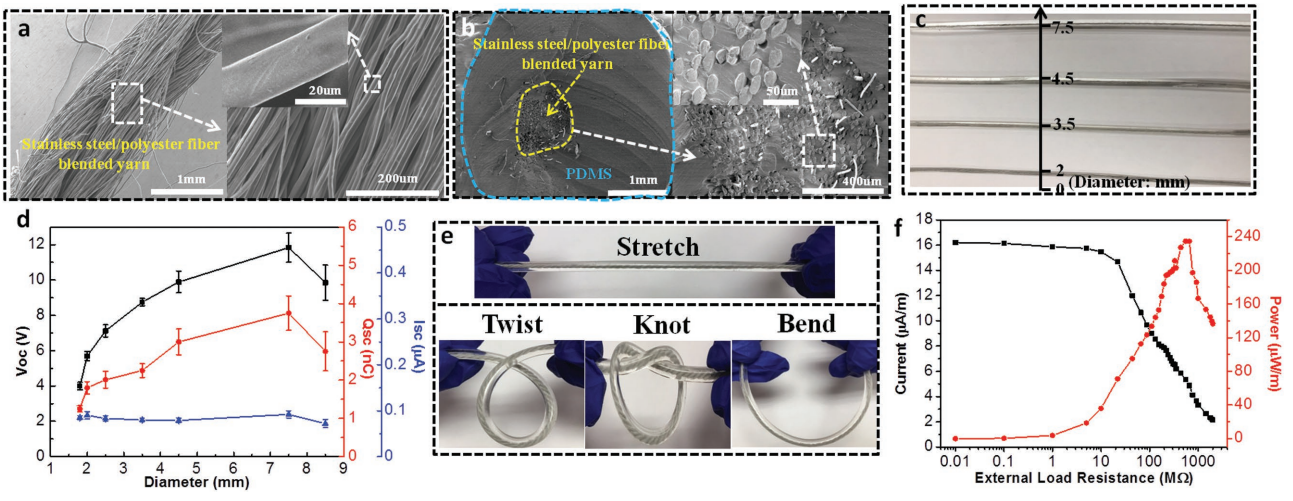

Figure 1. PDMS-coated energy-harvesting yarn. a) SEM images of 3-ply-twisted stainless steel/polyester fiber blended yarn with different magnifications. b) Cross-sectional SEM images of PDMS-coated energy-harvesting yarn with different magnifications. c) Photograph of energy-harvesting yarn with different PDMS-coated diameters. d) Dependence of OC voltage (V_{OC}), SC current (I_{SC}) and SC transferred charge (Q_{SC}) of energy-harvesting yarn on the PDMS-coated diameters. e) Photographs of as-prepared single PDMS-coated energy-harvesting yarn with demonstrations of being different mechanical forces including stretching, twisting, knotting, and bending. f) Dependence of SC current density and power density of PDMS-coated energy-harvesting yarn on the external load resistances under the tapping frequency of 3 Hz.

of the PDMS-coated yarns (1.8–8.5 mm, Figure 1c) were fabricated to compare their energy-harvesting capacities. Their basic power outputs were measured via the periodic contact and separation motions (Figure S2a, Supporting Information). The diameter-dependent electrical output results (open-circuit (OC) voltage V_{OC}, short-circuit (SC) current $I_{SC,}$ and short-circuit charge transfer Q_{SC} curves) were plotted in Figure 1d (Figure S2b–d, Supporting Information). It can be found that the V_{OC} and Q_{SC} of the energy-harvesting yarns were first increased with the increase of the diameter yet then decreased when the diameter exceeded 7.5 mm. The reason can be attributed to the variation of contact area between PDMS and external substrate.[40] At the beginning, the increase of diameter brings more contact area with the outside substrate, resulting in a higher power output. The contact area would achieve a maximum value when the diameter was close to 7.5 mm. Afterward, more increase in diameter would lead to the reduction of power output due to the reduced electrostatic induction effect. As a result, the diameter of 3.5 mm was chosen to weave the 3DOW-TENG after comprehensive evaluations of the power outputs and final fabric's thickness. The compatibility of this kind of yarn with the existing mature textile manufacturing technique is discussed (Note S3, Supporting Information). The output power of the energy-harvesting yarn was further investigated by externally connecting various loads from 10 kΩ to 2000 MΩ in series. The power was calculated as $I^2 R$, where I is the output current across the external load and R is the load resistance. The instantaneous power density under the tapping frequency of 3Hz achieved a peak value of 234.67 μW m^{-1} at a load resistance of 550 MΩ (Figure 1e). This flexible yet robust energy-harvesting yarn can also sustain various kinds of complex mechanical deformations, such as stretching, twisting, knotting, and bending (Figure 1f), which is suitable for fabricating the high-power-output energy-harvesting 3DOW-TENG.

In addition to the energy-harvesting yarn, the organizational structure of textiles also plays a significant role in the final electrical output performances. As demonstrated in the technical route (Figure S3, Supporting Information), our work originated from a 2D plain woven model. In a course of weaving a plain pattern, warp and weft yarns interweave every one yarn, and their movements form a simple crisscross intersection pattern. Due to its clear structure and simple weaving method, this 2D structure was commonly used in previous textile-based TENGs. Therefore, this kind of 2D plain woven TENG (one-dielectric-layer TENG in this paper) was first fabricated. It indicated that the increase of stacked layers led to the increase of power outputs.[41,42] Therefore, one more dielectric layer was added in the thickness direction of 2D plain woven structure to form a two-dielectric-layer TENG. According to the triboelectric effect, two materials with different electronegativity can generate more transferred charges during contact.[23,24] Therefore, a conductive layer was arranged between the two outer dielectric layers, which eventually contributed to the formation of the 3DOW-TENG. It is worth noting that the 3D orthogonal woven structure is also commonly used in the textile field, which has already been applied in various domains, and in the meantime, is suitable for high efficient production.

As illustrated in **Figure 2**a, the architecture of the 3DOW-TENG mainly consists of three different sets of yarns: 3-ply-twisted stainless steel/polyester fiber warp yarns forming the middle conductive layer, PDMS-coated energy-harvesting weft yarns forming the top and bottom dielectric layers, and nonconductive *Z*-yarns (also referred as warp-weaver or *Z*-binder) placed in the thickness direction forming the binding layers. On one hand, in the 3D orthogonal woven fabric, there is no interlacing between warp and weft yarns, and they are straight and perpendicular to each other. On the other hand, *Z*-yarns combine the warp and weft layers by interlacing (moving up and down) along the warp direction over the weft yarns. Interlacing only occurs on the top and bottom surfaces of the fabric. Based on the type of *Z*-yarn, the 3DOW-TENG can be divided into conductive or nonconductive (Figure 2b and Figure 2c, respectively). Each of the 3DOW-TENG has several types of circuit connection patterns, which directly affect their final power-output performances. In the following, we discussed the electrical output performances of different structures from three aspects, i.e., the type of *Z*-yarn, the number of stacked layers, and the circuit connection mode (Figure S3, Supporting Information).

The electrical outputs of conductive *Z*-yarn binding TENGs were first discussed. Based on the stacked layers, the conductive *Z*-yarn binding TENGs could be divided into one-dielectric-layer TENG (Figure S4, Supporting Information), two-dielectric-layer TENG (Figure S5, Supporting Information), and 3DOW-TENG (Figure S6, Supporting Information). The detailed discussion on the electrical output performances of one/two-dielectric-layer TENGs was also provided in Note S4 (Supporting Information). According to the circuit connection mode, the conductive *Z*-yarn binding 3DOW-TENG could be further divided into weft-connection single-electrode mode, weft–warp-parallel-connection single-electrode mode, and double-electrode mode. Based on the electrical output results of the three types of TENGs (Figures S4–S6, Supporting Information), several conclusions could be made. First, the electrical outputs of two-dielectric-layer TENG were higher than those of one-dielectric-layer TENG, whatever the circuit connection patterns are, clearly demonstrating that more dielectric layers contribute to higher power outputs. Second, for one-dielectric-layer or two-dielectric-layer TENG, the double-electrode mode showed the lowest electrical outputs as compared with other two connection modes. However, the results for 3DOW-TENG were opposite. The reason could be attributed to the surface-exposed conductive yarns, which decreased the charge transferred from the external substrate. It is well known that the ability of a material for gaining/losing electron depends on its polarity. Very few induced charges can be produced between two materials with similar triboelectric properties. In the TENG systems, most of the transferred charges come from external substrates or surfaces (for wearable textile, most of time is our skin), besides the contact-separation movements between warp and weft yarns. According to the triboelectric series,[23,24] the skin is easy to attain positive charges when approached, which is the same as most of metal materials. Therefore, the similar triboelectricity between our skin and the top conductive layer would greatly weaken the electrical generation capability of conductive *Z*-yarn binding TENGs, due to their low ability to acquire electrodes from our skin. Nevertheless, the surface-exposed conductive yarns in the 3DOW system were less than those in other two TENGs. Moreover, the contact

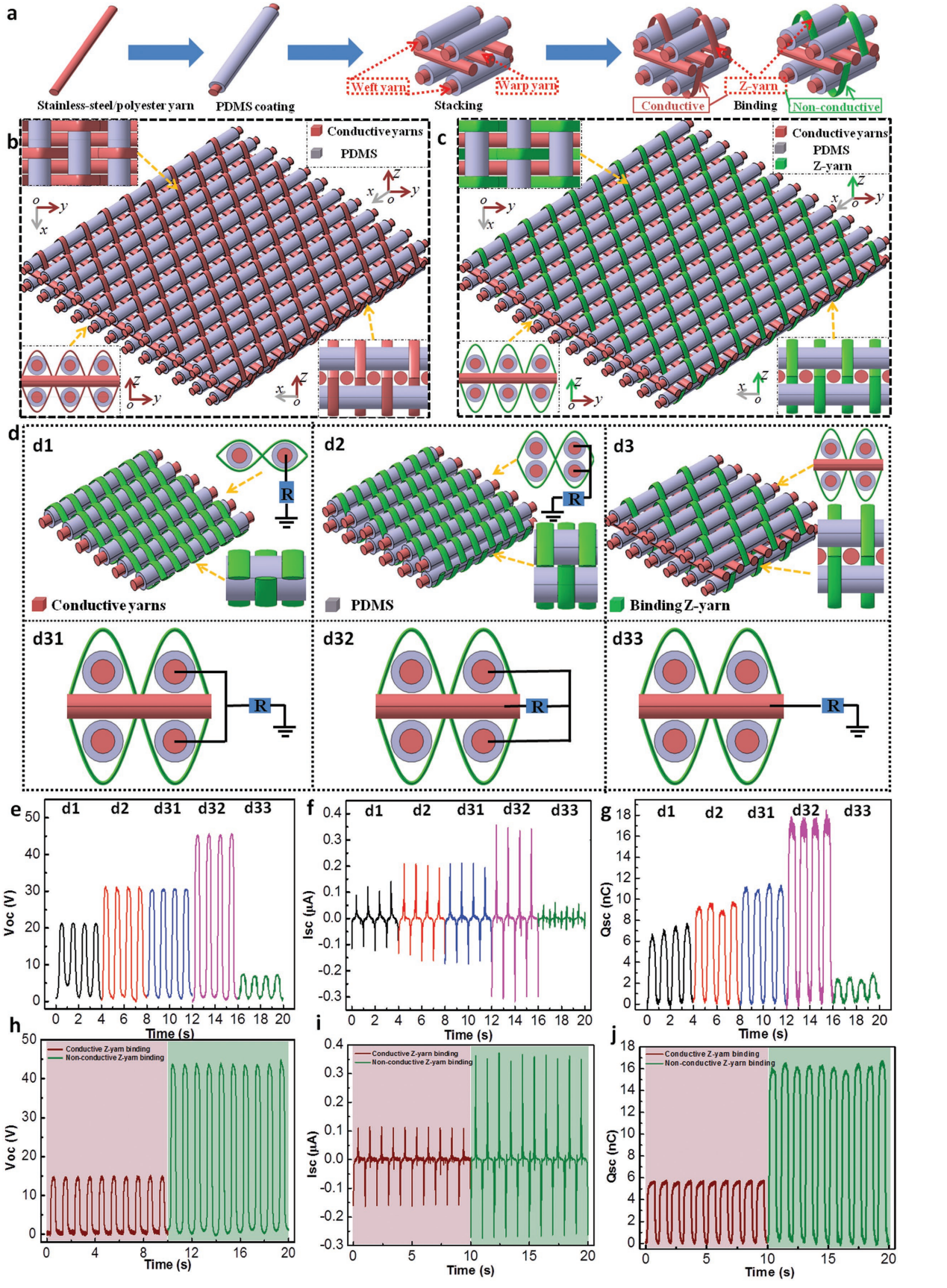

and separation movement between the added middle conductive layer and two outside dielectric layers would generate extra friction charges for 3DOW-TENG. The two factors contribute to a better power-output performance of 3DOW-TENG. To further verify the negative effects of surface-exposed conductive yarns on electrical generation, this article also fabricated a reversed 3DOW-TENG. By switching the position of conductive yarns and PDMS-coated yarns, a revised 3D orthogonal woven triboelectric nanogenerator (R-3DOW-TENG) could be obtained (Figure S7, Supporting Information). It was found that the R-3DOW-TENG generated much less output power in comparison with 3DOW-TENG, clearly demonstrating the negative influence of the surface-exposed conductive yarns. In this article, a detailed discussion on the electrical output performances of the R-3DOW-TENG was also provided in Note S5 (Supporting Information).

As indicated above, the surface-exposed conductive yarns had disadvantages of charges transferring, which should be substituted by nonconductive yarns. In analogy with conductive *Z*-yarn binding TENGs, the nonconductive *Z*-yarn binding TENGs also had three types, namely one-dielectric-layer TENG (Figure 2d1), two-dielectric-layer TENG (Figure 2d2), and 3DOW-TENG (Figure 2d3). The 3DOW-TENG could be further divided into weft-connection single-electrode mode (Figure 2d31), double-electrode mode (Figure 2d32), and warp-connection single-electrode mode (Figure 2d33) based on its circuit connection patterns. The electrical outputs of the six distinct patterns were shown and compared in Figure 2e–g. With more PDMS-coated yarns arranged in the weft direction, the two-dielectric-layer TENG showed better electrical output performances than one-dielectric-layer TENG. The weft-connection single-electrode 3DOW-TENG showed no obvious improvement (almost the same) comparing with the two-dielectric-layer TENG. In other words, the conductive warp yarns played no role in this connection mode. However, in the warp-connection single-electrode 3DOW-TENG, the conductive warp yarns could also generate a small amount of electrical outputs. In order to make a full use of the 3D structure, the double-electrode 3DOW-TENG was designed. Considering the extra contact-separation motion added between the middle conductive layer and two outside dielectric layers, the electrical generation capability of the double-electrode 3DOW-TENG could be greatly improved.

The comparisons of electrical outputs between conductive and nonconductive *Z*-yarn binding 3DOW-TENGs demonstrated that the nonconductive binding 3DOW-TENG generated nearly triple electrical outputs than the conductive *Z*-yarn binding 3DOW-TENG (Figure 2h–j). In a word, it was turned out that the nonconductive *Z*-yarn binding 3DOW-TENG with double-electrode mode possessed the best power-output performances. This remarkable improvement in power output was attributed to the optimum structural design by adding the double outer dielectric layers and the middle arrayed conductive layer into the fabric system. Therefore, in the following analyses and demonstrations, we only discussed this kind of TENG.

The working mechanisms of the fabricated 3DOW-TENG were schematically illustrated in **Figure 3**a. By taking the skin as an external surface, the relative motions could be simplified as two contact-separation processes that occurred between skin and top weft layer, top-bottom weft layers, and middle warp layer. In the original state (i), the PDMS surface was charged with negative electrostatic charges and the stainless steel electrode produced positive charges, due to electrostatic induction and conservation of charges. When the 3DOW-TENG was pressed by skin (ii), a shrinkage of the gap between the middle warp electrode layer and bilateral PDMS would result in induced positive charges accumulating in the middle conductive layer due to the electrostatic induction. Accordingly, free electrons in the middle conductive layer would flow to the two outer conductive layers to balance the electrostatic status. This process produced an instantaneous positive current. It was necessary to note that the charges on PDMS would not be annihilated even when it contacted the middle electrode layer (iii), because the electrostatic charges were naturally impregnated into the insulator PDMS. In the reverse case, when the 3DOW-TENG was released (iv), it would recover back to its initial state (i) and the internal gap would be recovered. Thus, an instantaneous negative current would be produced. As a result, a contact-separation process of the 3DOW-TENG would generate an instantaneous alternating current through the load. The above proposed working mechanisms could be well validated by our experimental results. As illustrated in Figure S8 (Supporting Information), one cycle of the contact-separation movement correspond to one cycle of electrical output curves; the details were discussed in Note S6 (Supporting Information). In this paper, a theoretical model of 3DOW-TENG was also established to simulate the electric potential distributions of every component at the contact and separation states by COMSOL software, as illustrated in Figure 3b.

The digital photographs of the test 3DOW-TENG sample (45×40 mm^2) were shown in Figure 3c. As illustrated in Figure 3d, a linear motor with a contact area of 15×15 mm^2 was used to trigger the 3DOW-TENG fabric, and the maximum movement distance between the external substrate and the 3DOW-TENG fabric was purposely set as 25 mm. As shown in Figure 3e–g, when the tapping frequencies varied from 0.5 to 5 Hz, the V_{OC} and Q_{SC} almost remained constant (45 V and 18 nC, respectively). However, the I_{SC} increased from 0.2 to 1.8 μA, revealing a clear increase trend with the increase in

Figure 2. Structure designs and electrical output comparisons of different TENGs. a) Fabrication processes of the 3DOW-TENG. b,c) Schematic representations of b) conductive and c) nonconductive *Z*-yarn binding 3DOW-TENG. The top left, bottom left, and bottom right are the partial enlarged front, top, and side view (three views) of the two 3DOW-TENGs, respectively. d) Schematic illustrations of nonconductive *Z*-yarn binding TENGs, including d1) one-dielectric-layer TENG, d2) two-dielectric-layer TENG, d3) 3DOW-TENG. According to the circuit connection patterns of this 3DOW-TENG, it can be further divided into d31) weft-connection single-electrode mode, d32) double-electrode mode, and d33) warp-connection single-electrode mode. e–g) Comparison of the electric output performances including e) OC voltage, f) SC current, and g) SC transferred charge of nonconductive *Z*-yarn binding TENGs. h–j) Comparison the electrical output performances including h) OC voltage, i) SC current, and j) SC transferred charge between conductive and nonconductive *Z*-yarn binding 3DOW-TENGs.

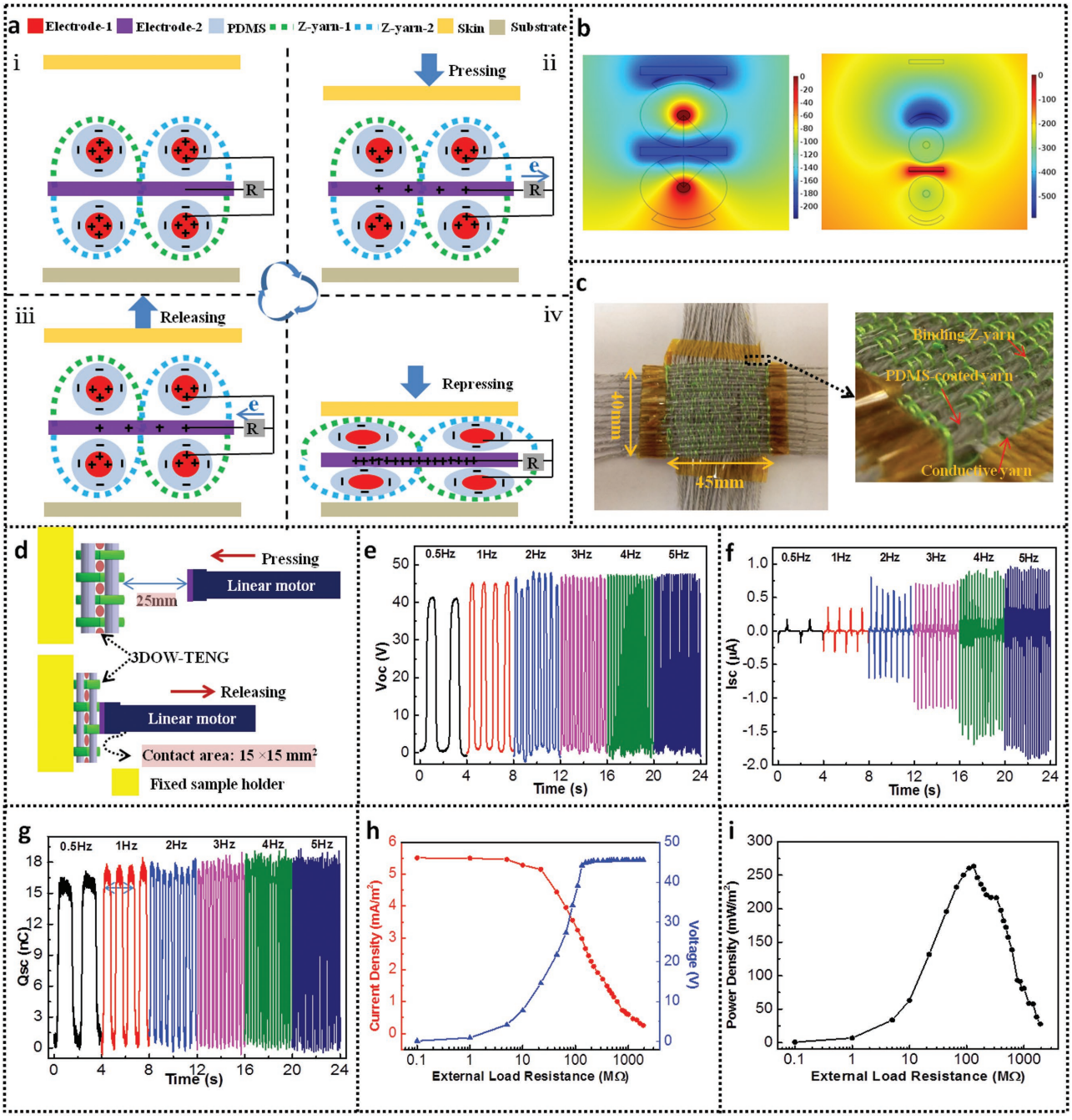

Figure 3. Working mechanism and electrical output performance of the nonconductive *Z*-yarn binding 3DOW-TENG. a) Schematic diagrams of the working principles of the 3DOW-TENG under contact-separation motion. b) Simulation results of the potential distribution of the 3DOW-TENG under open circuit condition by using COMSOL software. c) Photograph of the 3DOW-TENG with the surface area of 45 × 40 mm^2. d) Illustrations of the experiment setup with a contact-separation mode. e–g) Electrical outputs of the 3DOW-TENG at various motion frequencies (0.5–5 Hz), including e) V_{OC}, f) I_{SC}, and g) Q_{SC}. h,i) Output current density, h) voltage, i) and power density of the 3DOW-TENG at different external load resistances varied from 100 kΩ to 2000 MΩ with a tapping frequency of 3 Hz.

frequency. In other words, the increase in frequency was favorable for the magnitude of I_{SC}. At a fixed contact frequency of 3 Hz, the power densities of the 3DOW-TENG were investigated by connecting it in series with external variable resistors. It was found that the output voltage increased sharply with the increment of resistance from 100 kΩ to 220 MΩ, and subsequently saturated when the load resistance was further increased to 2000 MΩ. In contrast, the generated current followed a reversed trend versus the output voltage, as shown in Figure 3g. The peak power density of the 3DOW-TENG reached 263.36 mW m^{-2} under a load resistance of 132 MΩ (Figure 3h), as calculated by $p = I^2 R$. It was necessary to point out that

in our design the yarns of the same layer were connected in parallel. In order to analyze the influence of the connection method of the yarns in the same layer on final power outputs, the 3DOW-TENG with series connection of yarns was also fabricated (Figure S9a, Supporting Information). Almost the same or even less power outputs were found in Figure 3e–g and Figure S9b–d (Supporting Information), demonstrating that the connection method of yarns in the same layer had no notable influence on the final power outputs. The long-term durability of the 3DOW-TENG was also tested. As shown in Figure S10 (Supporting Information), almost no significant decrease was found after 1500 tapping cycles, clearly demonstrating the practical value of this stable and reliable energy-harvesting fabric.

A large-area energy-harvesting 3DOW-TENG (**Figure 4**a) was fabricated to demonstrate the multifunctional applications in our daily life. As shown in Figure 4b, the 3DOW-TENG could be worn in the forearm and simultaneously sustained various kinds of complex mechanical deformations, including stretching, folding, and crimping. Figure 4c showed that the 3DOW-TENG could power up 71 LEDs in series only by palm tapping (Movie S1, Supporting Information) or foot stepping (Movie S2, Supporting Information). By utilizing the vibration resulting from periodic movement of human body in the process of walking, a wearable and self-powered warning indicator was designed. When the wearer is walking in the dark night, it can be easily recognized by the approaching vehicles. Just as demonstrated in Figure 4d, the "STOP" sign with 16 LEDs hanged in the chest (Movie S3, Supporting Information) or behind the back (Movie S4, Supporting Information) could be lighted up by arm swinging. Furthermore, with the help of full-wave bridge rectifiers, the converting power generated from human body motion could also be stored in a capacitor or battery for later uses. As illustrated in Figure 4e, by hand tapping the 3DOW-TENG, a commercial capacitor of 0.68 μF could be charged to 2.5 V after 7 s. The stored electricity could sustainably drive an electronic watch, as demonstrated in Figure 4f and Movie S5 (Supporting Information). In these processes, it was necessary to point out that the watch started to work only when the voltage reached the threshold voltage. Although the voltage of capacitor quickly dropped after the threshold voltage, it would rise again if we continued tapping the fabric. It was indicated that our 3DOW-TENG could not only sufficiently drive the watch but also sustainably charge the capacitor/battery. These demonstrations manifested that the 3DOW-TENG could be used as a sustainable and body-adaptive power source for driving wearable gadgets.

Our 3DOW-TENG also shows potential applications in self-powered human-interactive and sensing devices. As illustrated in Figure 4g and Movie S6 (Supporting Information), by wearing the fabric on the forearm, a real-time arm swinging pattern of an individual was recorded with four different motion states (low, high, fast, and slow). The swinging amplitude and frequency of two indicators were selected to evaluate the capability of 3DOW-TENG in monitoring the body's behavior. When arm moved up and down within a low distance, the average swinging voltage was about 30 V, while for a high distance, the average voltage amplitude would reach about 125 V. The swinging frequency mainly affected the number of swinging per unit time, which had 141 times per minute for fast moving yet 48 times per minute for slow moving. This demonstrated that the wearable self-powered 3DOW-TENG was very useful and convenient for human motion tracking, considering no additional power required. For example, the training strength of an athlete can be constantly monitored according to the amplitude and frequency of the electrical signals motivated by his body or joint movements. In addition, in cooperation with signal-processing equipment and special weaving methods, the self-powered 3DOW-TENG can be utilized as an active sensor for more sophisticated and wireless applications. A novel self-powered textile was designed to fully harvest human walking energy and simultaneously perceive human motion signal. As illustrated in the top right view of Figure 4h, a self-powered dancing blanket was fabricated through weaving the energy-harvesting regions and nonconductive regions into a whole fabric. The operation status of this self-powered dancing carpet is shown in Figure 4h; that stepping on different energy-harvesting regions would actively motivate corresponding movements on the screen. In this article, how the self-powered dancing blanket works was also demonstrated. The dancing blanket was divided into nine rectangle energy-harvesting regions (45×40 mm^2). In each divided region, cotton yarns were sewn on their surface for presenting different indicative symbols. The simulated signal receiver was composed of nine LED sets, which were connected with the nine rectangle energy-harvesting regions with corresponding indicative symbols, respectively. When the mechanical forces were applied to the rectangle energy-harvesting regions, such as palm tapping in Figure 4i (Movie S7, Supporting Information) and foot stepping in Figure 4j (Movie S8, Supporting Information), the corresponding electrical indicators would be lighted. In the near future, with the assistance of information acquisitions and conversion equipment, our self-powered 3DOW-TENGs can be used as smart textiles for wireless intelligent unlocking and safeguard systems. For example, a door can be unlocked and opened by touching different positions of the smart carpet paved under the doorway. What is more, the intelligent carpet can also be applied in home security protection that it can give timely electrical signal feedback to the owner when a stranger enters a sensitive area.

As for textiles, washing durability is an essential basic requirement for their long-term usage. In our 3DOW-TENG fabric, on one hand, both of the stainless steel/polyester fiber blended yarn and the coated hydrophobic PDMS are washable. Little or ever no yarn shrinkage was found during the laundering process. On the other hand, the binding *Z*-yarn constructs regular constrain networks to the stacked warp and weft yarns, which can effectively resist any kind of complex mechanical agitation and internal deformation. In this work, the washability of 3DOW-TENG was tested by a simulated laundering environment (Figure S11a, Supporting Information) with household detergent and magnetic stir bar added to a beaker. Each laundering cycle lasted 20 min, and the spinning velocity of the magnetic stirrer was controlled to 600 rpm. After running each cycle and drying naturally, the power outputs after different times washing under a fixed tapping frequency of 4 Hz were measured (Figure S11b,c, Supporting Information). Furthermore, a long-term cyclic result, after washing ten times, was also presented (Figure S11d, Supporting Information). The

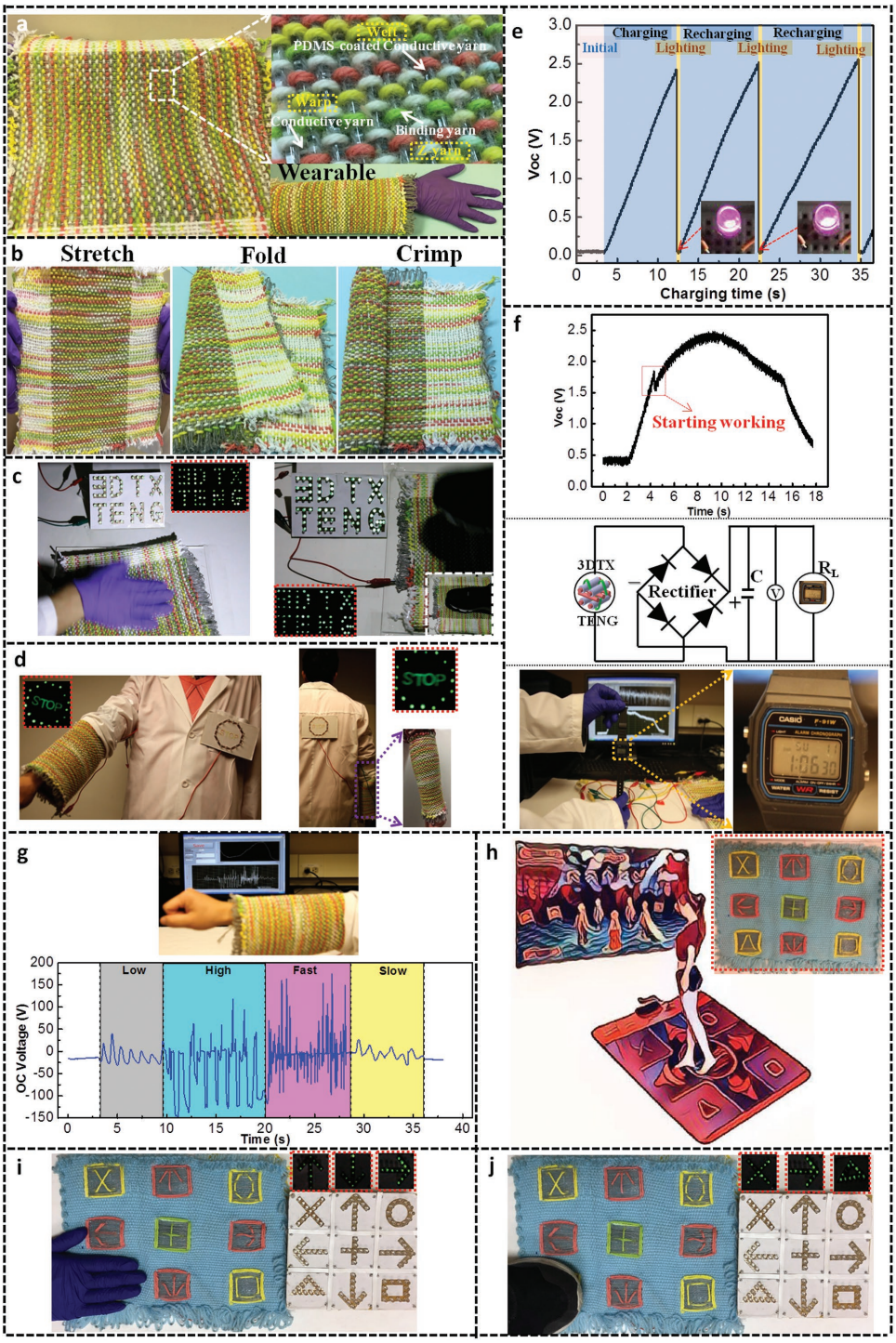

Figure 4. Digital photograph and demonstration of the large-area energy-harvesting 3DOW-TENG. a) Digital photographs of large-area wearable textile 3DOW-TENG. Top right view is the partial enlarged view of 3DOW-TENG, which shows its three components including stainless steel/polyester blended conductive warp yarn, PDMS-coated energy-harvesting weft yarn and binding *Z*-yarn. b) Photographs of 3DOW-TENG under various mechanical deformations, including stretching, folding, and crimping. c) Photograph demonstrating that the 3DOW-TENG can easily light up 71 LEDs with "3DTX TENG" displaying just by palm tapping (left) or foot stepping (right). d) Photograph demonstrating that the 3DOW-TENG can be used as a self-powered system for wearable night warning indicator. Just as the "STOP" symbol, for example, the self-powered 3DOW-TENG worn on the forearm can light up the 16 warning LEDs whether they were hanged in the chest (left) or behind the back (right). e) Charging capability of 3DOW-TENG by practical hand tapping on a commercial capacitor of 0.68 μF. f) Demonstration of continuously driving a smart watch by hand tapping on the 3DOW-TENG with power management circuit. g) OC voltage of a self-powered active 3DOW-TENG motion sensor worn on the forearm accompanied with four different motion states, including low, high, fast, and slow. h) Schematic diagram and digital photograph of the self-powered dancing blanket. i,j) Demonstrations of the dancing blanket that can be worked just by i) palm tapping or j) foot stepping.

capability to harvest mechanical energy was well maintained without any significant decline, clearly indicating its washability as well as robustness and stability. It was worth noting that our 3DOW-TENG fabric was washed without any encapsulation or packaging, and this simulated washing procedure provided the harshest test conditions for the unpackaged devices.

Our 3DOW-TENG fabric also possesses good comfortability when it is integrated into manufacturing production systems or even eventually worn on human bodies. As for textiles, the comfortability is primarily involved with two categories: heat–moisture comfort and tactile comfort. Heat–moisture comfort represents that fabric can maintain and regulate the temperature stability of human body and humidity suitability of microenvironment in the process of heat and humidity transference between human body and outer environment. It mainly includes heat insulation, warmth retention, permeability, heat/moisture transfer, and dissipation. As illustrated in Figure S12 (Supporting information), there is a certain amount of static air existing inside the fabric that makes our 3DOW-TENG fabric possess excellent warmth retention. The permeability of fabrics includes air permeability, moisture penetrability, water permeability, and light transmission. Because the spaces between the yarns form many flowing channels/bridges that connect human skin with outer environment (Figure S12, Supporting information), the air, moisture, water, heat, and light are easy to get through these channels/bridges when there is any environmental difference existing between human skin and outer environment. For example, the heat and sweat generating from human body can be transported to outer environment through these channels when an individual feels hot. On the contrary, when an individual feels cold or dry, the heat or moisture from the outer environment will be delivered through these channels to human body. The *Z*-binding cotton yarns also play a role in absorbing the sweat of human skin or moisture in the environment to balance the humidity between human skin and outer environment (Figure S12, Supporting information). It is worth noting that the permeability of our fabric can be well adjusted by selecting appropriate diameters and arrangement densities of warp and weft yarns, according to actual requirements. Tactile comfort is primarily concerned with prickle sensation, fabric weight, static electricity, and cold stimulation. The blended conductive yarn almost maintains the properties of regular polyester yarn, which is tactile soft, mechanical strong, and excellent resilience. The hydrophobic, biocompatible, and temperature-insensitive PDMS endows the energy-harvesting yarn with good waterproof and human friendly properties. Moreover, the low Young's modulus of PDMS leads to the good structural flexibility and easy deformability of our fabric. The three-layered structural design provides a moderate thickness and weight for our fabric with no excessive pressure to human skin. The excellent conductivity of stainless steel/polyester fiber blended yarn can effectively prevent the electrostatic charge accumulation on the surface of our fabric. The main reason resulting in cold stimulation of fabric is the moisture and water absorption of fiber. In our 3DOW-TENG fabric, both the blended yarn and PDMS are hydrophobic, so they can reduce the moisture and water absorption. Although the cotton yarn has slightly higher moisture regain (≈8.5%) compared with its counterparts, its volume fraction in our 3DOW-TENG is so less that its effect can be ignored. In addition, the comfortability of our fabricated textile can be further improved by the textile finishing process, such as softening finishing, crease resistance finishing, and so on.

In summary, a washable, deformable, breathable, and comfortable 3DOW-TENG with high-power-output performance and long-term durability is fabricated. After comparing with various structures and different circuit connection patterns, the nonconductive *Z*-yarn binding 3DOW-TENG with double-electrode mode is proved to be the optimized structural design in the power-output performance. Besides, the electrical generation mechanism and power-output performance of this novel 3D textile structure were discussed in detail. The advanced 3D orthogonal structure provides enough contact-separation space for the stainless steel/polyester fiber blended conductive yarns and the PDMS-coated energy-harvesting yarns, of which the maximum peak power density can reach 263.36 mW m^{-2} under the tapping frequency of 3 Hz. Furthermore, the wearable textile 3DOW-TENG has been demonstrated for a broad range of applications, such as lighting up a warning indicator, charging a commercial capacitor, driving a digital watch, and tracking human motion signals. Moreover, a self-powered dancing blanket is designed for harvesting human walking energy and capturing human motion signals at the same time. In future, this smart carpet can be used in home security protection and intelligent unlocking system. Our work introduces a novel 3D orthogonal woven structure into the development of high-power-output wearable textile TENGs and verifies its promising applications in both biomechanical energy harvesting and self-powered sensing.

Experimental Section

Preparation of Energy-Harvesting Yarn: Commercial 3-ply-twisted stainless steel/polyester fiber (20 and 80 wt%, respectively) blended yarn (Sparkfun electronics) as the electrode was inserted into a circular plastic tube. The two ends of the plastic tube were sealed by circular acrylic panels with epoxy resin glue. In the center of the circular acrylic panels, a hole was reserved for inserting the yarn. Second, the tube was placed along the gravitational direction which can make the yarns placed in the center of the tube perfectly. Then the upper and lower ends of the yarn were fixed with the upper and lower clamps, respectively. PDMS (Sylgard 184, Dow Corning) as a dielectric material was prepared by mixing the base monomers and the curing agent with the ratio of 10:1 by weight. After mixing, the solution of PDMS was degassed in vacuum for 30 min to thoroughly remove the bubbles. Afterward, the solution of the prepared PDMS was syringed into the tube along the tube wall to slowly fill the tube. After about 10 h, the tube was put on an oven where the PDMS got slightly viscous. After curing 2 h at 80 °C, the energy-harvesting yarn could be obtained by removing the circular plastic tube.

Fabrication of Energy-Harvesting 3DOW-TENG: Although the 3DOW-TENG was woven by hand in a self-designed mold in this work, its mature manufacturing technique had already existed in the textile field, which was suitable for large-area industrial production. The specific fabricating methods were as follows: the PDMS-coated energy-harvesting yarns were first arranged in the weft direction of the mold as the bottom layer; afterward, the stainless steel/polyester fiber blended yarns were arranged in the warp direction as the middle layer; then the PDMS-coated energy-harvesting yarns were arranged again in the weft direction as the top layer. Finally, the *Z*-directional yarns (conductive or nonconductive) interwove with weft yarn one by one along the warp direction to bind the 3D fabric to a whole. In this 3DOW-TENG, the air

permeability could be adjusted by rational designing the spatial density of warp, weft, and *Z*-directional yarns in the weaving process.

Washing Test: The simulated washing environment with household detergent and magnetic stir bar added was first cultivated in a beaker. Then, the textile 3DOW-TENG was directly put into the washing solution without any packaging. The prepared beaker was placed on the magnetic stirrer to imitate the roller rotation of the household washing machine. The spinning speed of magnetic stirrer was set as 600 rpm, and the whole washing process lasted for 20 min. Finally, the textile 3DOW-TENG was dried fast in the oven at 60 °C for later measurement.

Device Characterizations: The surface morphology of the conductive yarn and the cross section of the PDMS-coated energy-harvesting yarn were characterized by field emission scanning electron microscope (SU-8010, Hitachi). For the measurement of the electrical output capability of the 3DOW-TENG, external forces were applied by a commercial linear mechanical motor, which corresponded to the stretching and releasing operations, respectively. The applied force was measured by Vernier LabQuest Mini. The OC voltage (V_{OC}), SC current (I_{SC}), and short-circuit (SC) transferred charge (Q_{SC}) were measured by an electrometer (Keithley 6541 System). The diameter of the PDMS-coated energy-harvesting yarn was measured by an electronic digital micrometer (733 Series Electronic Digital Micrometers, L. S. Starrett).

Supporting Information

Supporting Information is available from the Wiley Online Library or from the author.

Acknowledgements

K.D., J.D., and Y.Z. contributed equally to this work. The authors are grateful for the support received from the "Thousands Talents" program for pioneer researcher and his innovation team in China, the Presidential Funding of the Chinese Academy of Science, and the National Natural Science Foundation of China (Grants Nos. 51432005, 5151101243, and 51561145021). K.D. and J.D. thank the China Scholarship Council for supporting research at the Georgia Institute of Technology, USA and the fundamental Research Funds for the Central Universities, China (Grant No. 170310103).

Conflict of Interest

The authors declare no conflict of interest.

Keywords

active motion sensors, biomechanical energy harvesting, triboelectric nanogenerators

Received: May 11, 2017
Revised: June 28, 2017
Published online:

[1] P.-C. Hsu, A. Y. Song, P. B. Catrysse, C. Liu, Y. Peng, J. Xie, S. Fan, Y. Cui, *Science* **2016**, *353*, 1019.
[2] J. Y. Oh, S. Rondeau-Gagne, Y. C. Chiu, A. Chortos, F. Lissel, G. N. Wang, B. C. Schroeder, T. Kurosawa, J. Lopez, T. Katsumata, J. Xu, C. Zhu, X. Gu, W. G. Bae, Y. Kim, L. Jin, J. W. Chung, J. B. Tok, Z. Bao, *Nature* **2016**, *539*, 411.
[3] R. L. Truby, J. A. Lewis, *Nature* **2016**, *540*, 371.
[4] A. Maziz, A. Concas, A. Khaldi, J. Stålhand, N.-K. Persson, E. W. Jager, *Sci. Adv.* **2017**, *3*, e1600327.
[5] Y. Qin, X. Wang, Z. L. Wang, *Nature* **2008**, *451*, 809.
[6] J. Chen, Y. Huang, N. Zhang, H. Zou, R. Liu, C. Tao, X. Fan, Z. L. Wang, *Nat. Energy* **2016**, *1*, 16138.
[7] Z. Wen, M. H. Yeh, H. Guo, J. Wang, Y. Zi, W. Xu, J. Deng, L. Zhu, X. Wang, C. Hu, L. Zhu, X. Sun, Z. L. Wang, *Sci. Adv.* **2016**, *2*, e1600097.
[8] K. Cherenack, C. Zysset, T. Kinkeldei, N. Munzenrieder, G. Troster, *Adv. Mater.* **2010**, *22*, 5178.
[9] Y.-D. Lee, W.-Y. Chung, *Sens. Actuator, B* **2009**, *140*, 390.
[10] S. Imani, A. J. Bandodkar, A. M. Mohan, R. Kumar, S. Yu, J. Wang, P. P. Mercier, *Nat. Commun.* **2016**, *7*, 11650.
[11] Y.-C. Lai, J. Deng, S. L. Zhang, S. Niu, H. Guo, Z. L. Wang, *Adv. Funct. Mater.* **2017**, *27*, 1604462.
[12] P. K. Yang, L. Lin, F. Yi, X. Li, K. C. Pradel, Y. Zi, C. I. Wu, J. H. He, Y. Zhang, Z. L. Wang, *Adv. Mater.* **2015**, *27*, 3817.
[13] F. Yi, X. Wang, S. Niu, S. Li, Y. Yin, K. Dai, G. Zhang, L. Lin, Z. Wen, H. Guo, *Sci. Adv.* **2016**, *2*, e1501624.
[14] W. Weng, P. Chen, S. He, X. Sun, H. Peng, *Angew. Chem., Int. Ed.* **2016**, *55*, 6140.
[15] M. K. Choi, J. Yang, K. Kang, D. C. Kim, C. Choi, C. Park, S. J. Kim, S. I. Chae, T. H. Kim, J. H. Kim, T. Hyeon, D. H. Kim, *Nat. Commun.* **2015**, *6*, 7149.
[16] K. Nomura, H. Ohta, A. Takagi, T. Kamiya, M. Hirano, H. Hosono, *Nature* **2004**, *432*, 488.
[17] Y. C. Lai, J. Deng, S. Niu, W. Peng, C. Wu, R. Liu, Z. Wen, Z. L. Wang, *Adv. Mater.* **2016**, *28*, 10024.
[18] W. Zeng, L. Shu, Q. Li, S. Chen, F. Wang, X. M. Tao, *Adv. Mater.* **2014**, *26*, 5310.
[19] X. Pu, L. Li, H. Song, C. Du, Z. Zhao, C. Jiang, G. Cao, W. Hu, Z. L. Wang, *Adv. Mater.* **2015**, *27*, 2472.
[20] J. Ren, Y. Zhang, W. Bai, X. Chen, Z. Zhang, X. Fang, W. Weng, Y. Wang, H. Peng, *Angew. Chem., Int. Ed.* **2014**, *53*, 7864.
[21] J. Bae, M. K. Song, Y. J. Park, J. M. Kim, M. Liu, Z. L. Wang, *Angew. Chem., Int. Ed.* **2011**, *50*, 1683.
[22] Z. Chai, N. Zhang, P. Sun, Y. Huang, C. Zhao, H. J. Fan, X. Fan, W. Mai, *ACS Nano* **2016**, *10*, 9201.
[23] Z. L. Wang, *ACS Nano* **2013**, *7*, 9533.
[24] Z. L. Wang, J. Chen, L. Lin, *Energy Environ. Sci.* **2015**, *8*, 2250.
[25] Y. Xie, S. Wang, S. Niu, L. Lin, Q. Jing, J. Yang, Z. Wu, Z. L. Wang, *Adv. Mater.* **2014**, *26*, 6599.
[26] Z. Zhao, X. Pu, C. Du, L. Li, C. Jiang, W. Hu, Z. L. Wang, *ACS Nano* **2016**, *10*, 1780.
[27] X. Wang, S. Niu, Y. Yin, F. Yi, Z. You, Z. L. Wang, *Adv. Energy Mater.* **2015**, *5*, 1501467.
[28] X. Wang, S. Niu, F. Yi, Y. Yin, C. Hao, K. Dai, Y. Zhang, Z. You, Z. L. Wang, *ACS Nano* **2017**, *11*, 1728.
[29] Z. Zhao, C. Yan, Z. Liu, X. Fu, L. M. Peng, Y. Hu, Z. Zheng, *Adv. Mater.* **2016**, *28*, 10267.
[30] K. N. Kim, J. Chun, J. W. Kim, K. Y. Lee, J.-U. Park, S.-W. Kim, Z. L. Wang, J. M. Baik, *ACS Nano* **2015**, *9*, 6394.
[31] T. Zhou, C. Zhang, C. B. Han, F. R. Fan, W. Tang, Z. L. Wang, *ACS Appl. Mater. Interfaces* **2014**, *6*, 14695.
[32] H. Sun, X. You, J. Deng, X. Chen, Z. Yang, J. Ren, H. Peng, *Adv. Mater.* **2014**, *26*, 2868.
[33] S. Kim, M. K. Gupta, K. Y. Lee, A. Sohn, T. Y. Kim, K. S. Shin, D. Kim, S. K. Kim, K. H. Lee, H. J. Shin, D. W. Kim, S. W. Kim, *Adv. Mater.* **2014**, *26*, 3918.
[34] X. He, Y. Zi, H. Guo, H. Zheng, Y. Xi, C. Wu, J. Wang, W. Zhang, C. Lu, Z. L. Wang, *Adv. Funct. Mater.* **2017**, *27*, 1604378.

[35] Z. Yang, J. Deng, X. Chen, J. Ren, H. Peng, *Angew. Chem., Int. Ed.* **2013**, *52*, 13453.
[36] Y. Yang, M. C. Gupta, K. L. Dudley, R. W. Lawrence, *Adv. Mater.* **2005**, *17*, 1999.
[37] C. Wu, T. W. Kim, F. Li, T. Guo, *ACS Nano* **2016**, *10*, 6449.
[38] W. Seung, M. K. Gupta, K. Y. Lee, K.-S. Shin, J.-H. Lee, T. Y. Kim, S. Kim, J. Lin, J. H. Kim, S.-W. Kim, *ACS Nano* **2015**, *9*, 3501.
[39] Z. L. Wang, L. Lin, J. Chen, S. Niu, Y. Zi, *Triboelectric Nanogenerators*, Springer International Publishing, Berlin, Heidelberg, Germany **2016**.
[40] S. Niu, Y. Liu, S. Wang, L. Lin, Y. S. Zhou, Y. Hu, Z. L. Wang, *Adv. Funct. Mater.* **2014**, *24*, 3332.
[41] Y. Xie, S. Wang, S. Niu, L. Lin, Q. Jing, Y. Su, Z. Wu, Z. L. Wang, *Nano Energy* **2014**, *6*, 129.
[42] P. Bai, G. Zhu, Z.-H. Lin, Q. Jing, J. Chen, G. Zhang, J. Ma, Z. L. Wang, *ACS Nano* **2013**, *7*, 3713.